Measurement of Open b Production at HERA

Daniel Pitzl

DESY, Notkestrasse 85, D-22609 Hamburg, Germany

Abstract. H1 and ZEUS have reported the first measurements of open b photoproduction at HERA. Both experiments use semi-leptonic decays to enrich a two-jet sample with heavy quarks. The beauty fraction is extracted from a fit of the measured p_T^{rel} distribution with contributions from b, c and light quarks according to a leading order QCD simulation. The measured cross section for b quarks is found to be larger than the predictions from next-to-leading order perturbative QCD calculations.

1 Introduction

The production of heavy quarks at HERA is an important testing ground for perturbative QCD calculations, where the heavy quark mass provides a hard scale. The basic mechanism, in leading order, is photon-gluon fusion, where a photon emitted from the electron and a gluon from the proton generate a heavy quark-antiquark pair. The dominant contribution to the cross section is due to the exchange of an almost real photon, whose negative squared four-momentum $Q^2 = -q^2$ is small. In this photoproduction regime, a second production mechanism becomes important, where the photon fluctuates into a hadronic state which is resolved into its partonic composition in the hard collision. In next-to-leading order QCD, however, only the sum of direct and resolved processes is unambiguously defined [1].

Heavy quark production at HERA is dominated by charm, with a total cross section of about $1\,\mu$b. The prediction for open b production is 3.8 nb from the leading order AROMA [2] Monte Carlo event generator, which uses massive matrix elements and considers direct processes only. Predictions from next-to-leading order QCD calculations [3–5] are between 4.7 nb and 10 nb, depending on the mass of the b quark and the parton distribution functions used.

During the years 1994 to 1997 HERA provided positron-proton collisions at a center of mass energy $\sqrt{s} = 300\,\mathrm{GeV}$. In photoproduction the photon-proton center of mass energy is given by $W_{\gamma p} \approx \sqrt{ys}$, where the proton mass has been neglected, and the inelasticity y is given by $y = q \cdot P / l \cdot P$, with P and l for the four momenta of the incoming proton and positron, respectively.

In the analyses of both H1 and ZEUS heavy quarks are identified by their semileptonic decays, which suppresses the light quark background. The flight directions of the quarks are approximated by reconstructing two jets in the final state. The contributions from b and c quarks are distinguished statistically by exploiting the effects of the higher b quark mass on the kinematics of the final state.

2 H1 muon analysis

The first measurement of the open b photoproduction cross section at HERA was reported by the H1 collaboration [6]. The final analysis [7] uses a data sample corresponding to an integrated luminosity of $6.6\,\mathrm{pb}^{-1}$ collected in 1996. The virtuality of the exchanged photon was restricted to the range $Q^2 < 1\,\mathrm{GeV}^2$ by requiring that no scattered positron candidate was found in the electromagnetic liquid argon or scintillating-fibre calorimeters. The variable y was calculated from a combination of calorimetric and tracking information using the Jacquet-Blondel method [8] and was required to be in the range $0.1 < y < 0.8$, corresponding to $95\,\mathrm{GeV} < W_{\gamma p} < 269\,\mathrm{GeV}$. The event selection required at least two jets in the pseudorapidity range $|\eta| < 2.5$ with transverse energies $E_T > 6\,\mathrm{GeV}$. The jets were identified using a cone algorithm with a radius $r = \sqrt{(\Delta\eta)^2 + (\Delta\phi)^2} < 1$, where η is the pseudorapidity and ϕ is the azimuthal angle of the track or cluster.

At least one muon candidate with a transverse momentum $p_t > 2\,\mathrm{GeV/c}$ had to be identified in the instrumented iron system in the polar angle range $35^o < \theta < 130^o$. The muon candidate had to be found within one of the jets. This sample contains muons from semi-leptonic decays of b and c hadrons and background from light quark decays and from hadrons faking a muon signature in the detector. A detailed and extensive Monte Carlo simulation was performed to determine the probability $\mathcal{P}_h^\mu(p,\theta)$ that a hadron $h = \pi, K$, or p produces a muon signature. These probabilities vary with momentum and polar angle but do not exceed 0.6% for pions, 2% for kaons and 0.2% for protons. They were tested using reconstructed decays of K_S^0 and ϕ mesons as sources of charged pions and kaons in the data. Figure 1 shows the distribution of pions from K_S^0 decays that produce a muon signature. It is well described, in shape and magnitude, by the muon fake probability for pions as obtained from the simulation. From the ϕ decays, eight kaons produced a muon signature, compared to an expectation of 7.8.

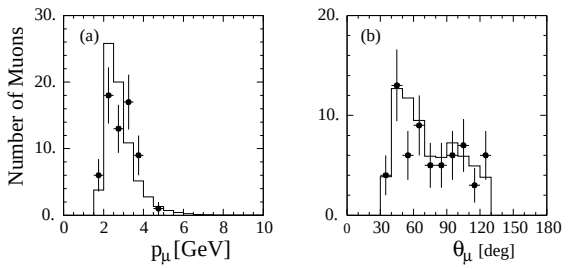

Fig. 1. Pions from K_S^0 decays producing a muon signature in the data (symbols with error bars) and the expectation from the muon fake probability $\mathcal{P}_\pi^\mu(p,\theta)$ (solid histogram).

The decay of a b hadron releases an energy of around 3 GeV and can involve decay particles with transverse momenta up to 2.3 GeV/c relative to the b hadron direction. The b hadron direction was experimentally approximated by the thrust axis of the jet, defined as the axis which maximizes

$$T = \max \frac{\sum_{i \neq \mu} |p_i^L|}{\sum_{i \neq \mu} |p_i|},$$

where the sum is over all particles in the jet except the muon. The transverse momentum of the muon relative to the thrust axis $p^{\mu}_{T,rel}$ was used to statistically separate b, c and light quark contributions in the sample. The $p^{\mu}_{T,rel}$ distribution for the 1996 H1 data is shown in figure 2. It has a maximum at about 0.7 GeV/c and a tail out to 4 GeV/c.

The $p^{\mu}_{T,rel}$ distribution of hadrons faking a muon signature was determined in shape and absolute normalization from a data sample of similar two-jet events, selected without the requirement of a muon candidate. The muon-fake probabilities $\mathcal{P}^{\mu}_{h}(p,\theta)$ were then applied to all particles in the jets, with a pion-kaon-proton ratio as given by the JETSET fragmentation model. The predicted background amounted to 25.9%. The expected shapes of the $p^{\mu}_{T,rel}$ distributions for b and c decays were taken from the AROMA Monte Carlo and the normalizations were determined from a fit to the data as $(50.8 \pm 4.9)\%$ for b and $(22.4 \pm 5.0)\%$ for c, where the errors are statistical only. The sum of the three contributions is in good agreement with the measured distribution.

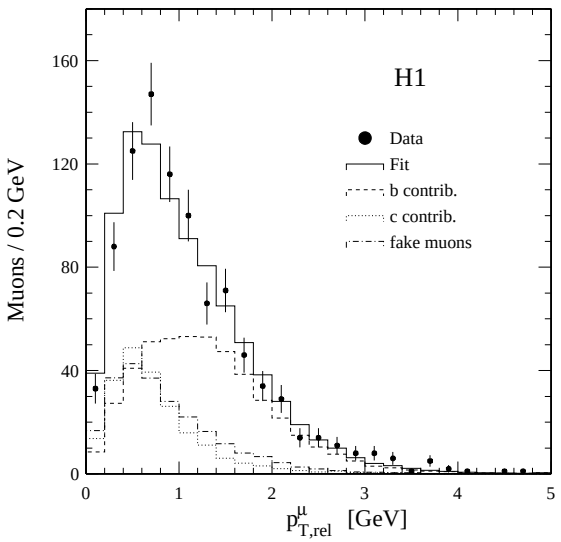

Fig. 2. The $p^{\mu}_{T,rel}$ distribution as measured by H1 (points with statistical error bars). The solid line is the sum of the fixed hadron background and the beauty and charm contributions from AROMA with normalizations from a fit to the data.

From the number of muons attributed to b events the cross section for open b production in the range $Q^2 < 1\,\mathrm{GeV}^2$, $0.2 < y < 0.8$, $p_T^\mu > 2\,\mathrm{GeV/c}$ and $35^o < \theta^\mu < 130^o$ was determined as

$$\sigma_{vis}(ep \to b\bar{b}X \to \mu Y) = \left(0.176 \pm 0.016\ (stat.)\ ^{+0.026}_{-0.017}\ (syst.)\right)\ \mathrm{nb}.$$

This cross section contains an extrapolation to the full phase space for the two jets, where the AROMA Monte Carlo gives an acceptance of 42.9% for the requirement of two jets with $E_T > 6\,\mathrm{GeV}$. The systematic error contains contributions due to uncertainties in the muon reconstruction efficiency, the hadronic energy scale in the calorimeter, and the luminosity determination. The systematic error due to the light quark background was determined by varying the fractions for pion, kaon and proton production and by using different data samples. The analysis was also performed using the HERWIG [17] and RAPGAP [10] leading order Monte Carlo Generators, which also contain resolved photon contributions. The effects of fragmentation was studied by varying the parameter ϵ of the Peterson fragmentation function. The variation of the cross section with different simulations amounts to $\pm 7.1\%$ and is included in the systematic error. The cross section predicted by AROMA in leading order and for direct photon processes only is 0.038 nb, where a b-quark mass of $4.75\,\mathrm{GeV/c^2}$ and the MRS-G [9] parton densities for the proton were used.

The measured cross section was compared to a next-to-leading order QCD calculation by the authors of [11]. Their program generates a final state at the parton level. In order to apply the cuts on the muon that define the visible cross section, the fragmentation and weak decay processes had to be added [7]. The b-quark mass was taken as $4.75\,\mathrm{GeV/c^2}$ and the MRS-G [9] and GRV-HO [12] parton densities for the proton and photon, respectively, were used. The cross section from the NLO QCD calculation in the kinematic range defined above was (0.104 ± 0.017) nb, where the uncertainty is due to the fragmentation process and a variation of the renormalization and factorization scales by a factor of two from the default value $\mu_R = \mu_F = \sqrt{m_b^2 + p_{t,b}^2}$. The NLO QCD prediction for the open b visible photoproduction cross section is 2.5 standard deviations below the measured value, where statistical, systematic and theoretical uncertainties were added in quadrature.

Nevertheless, the NLO QCD calculation [11] was used to extrapolate to the full kinematic phase space and to derive the total photoproduction cross section for b-quarks. The total branching ratio for a muon to be produced in the decay chain of b hadrons was applied. The Weizsäcker-Williams approximation was used to determine the equivalent flux of photons emitted by the positron. The average photon-proton center of mass energy is $\langle W_{\gamma p} \rangle \approx 180\,\mathrm{GeV}$. The measured cross section is

$$\sigma(\gamma p \to b\bar{b}X) = (111 \pm 10^{+16}_{-11} \pm 17)\ \mathrm{nb},$$

where the first and second error are the experimental statistical and systematic error and the third error is due to the extrapolation procedure and the uncertainty in the semileptonic branching ratio of B hadrons. The H1 measurement

is shown in figure 3 together with the NLO QCD prediction and a measurement by EMC [13] at fixed target energy.

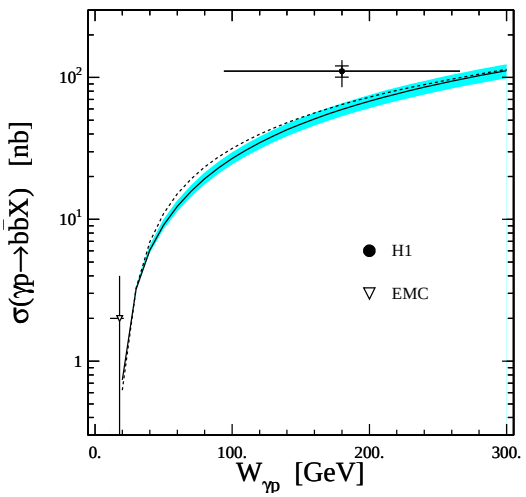

Fig. 3. The total photoproduction cross section $\sigma(\gamma p \to b\bar{b}X)$. The inner error bar is statistical while the outer error bar includes all systematic errors as explained in the text. The horizontal bar indicates the range of the measurement. The solid curve shows the NLO QCD calculation [11] and the shaded band indicates a change in the factorization scale by a factor of two. The dashed line shows the NLO prediction when the MRST [14] instead of the MRS-G [9] parton densities for the proton are used.

3 ZEUS electron analysis

The ZEUS collaboration has reported a measurement of the b production cross section using decays into electrons [15]. The data were collected during 1996 and 1997 when HERA was running with positrons. The integrated luminosity amounts to $36.9\,\mathrm{pb}^{-1}$. The kinematic range in the analysis was restricted to the region $Q^2 < 1\,\mathrm{GeV}^2$ and $0.2 < y < 0.8$.

The k_T clustering algorithm [16] was used to reconstruct jets and at least two jets with $E_T^{jet1} > 7\,\mathrm{GeV}$ and $E_T^{jet2} > 6\,\mathrm{GeV}$ in the pseudorapidity range $|\eta^{jet}| < 2.4$ were required.

Electrons were identified by using information from the central drift chamber and the uranium-scintillator calorimeter. A transverse momentum $p_T^{e^-} > 1.6\,\mathrm{GeV/c}$ was required and the pseudorapidity was restricted to the range $|\eta^{e^-}| < 1.1$. The specific energy loss dE/dx in the drift chamber is about 1.4 mip

for electrons due to the relativistic rise, while hadrons are minimum ionizing. Tracks were linked to calorimeter clusters, where a cluster is called electron enriched if it has more than 90% of its energy deposited in the electromagnetic section. Conversely, a cluster is called hadron enriched if it has more than 60% of its energy deposited in the hadronic section. The hadron enriched sample contains essentially no electrons and can be used as a background sample.

Figure 4 shows the dE/dx spectra of the electron and hadron enriched samples. The shaded region $dE/dx < 1.1$ mips is used for normalization. The lower part of figure 4 shows the subtraction of the two samples with a clear electron signal. A background of electrons from photon conversions in the material in front of the drift chamber is determined from the data and the detector simulation and is also shown in figure 4.

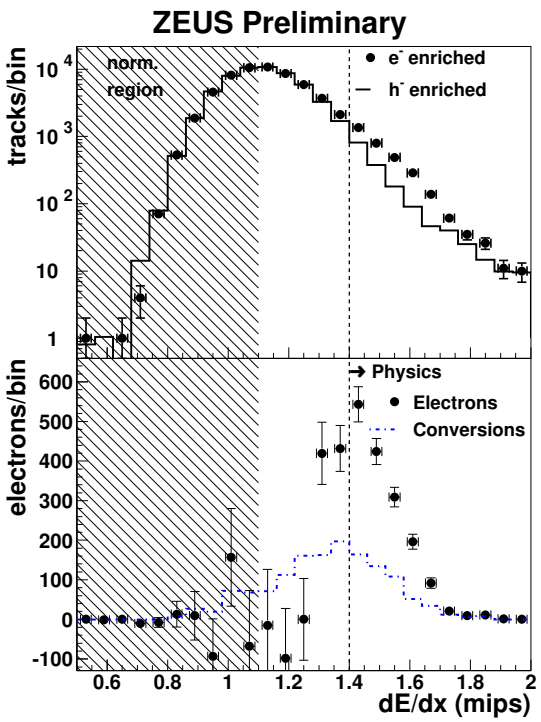

Fig. 4. (top) The dE/dx distributions for the electron enriched and the hadron enriched samples, normalized in the region dE/dx < 1.1 mips. (bottom) The subtraction shows the electron signal. The background from photon conversions is indicated by the dashed-dotted line.

The differential cross section $d\sigma/dp_{T,rel}$, where $p_{T,rel}$ is the transverse momentum of the electron relative to the closest jet, has been measured for the process $e^+ p \to$ dijet $e^- X$ and is shown in figure 5. The ZEUS data points show

the statistical error as the inner error bar and the statistical and systematic errors added in quadrature as the outer bars. The uncertainty due to the ZEUS calorimeter energy scale is shown separately as the shaded band. Figure 5 also shows the prediction from the HERWIG [17] leading order Monte Carlo program for beauty production (17%), for charm and light quarks (83%) and their sum. The overall rate was scaled by a factor of 3.7 in order to match the measured cross section. The HERWIG program was used with the default heavy quark masses ($m_c = 1.55\,\mathrm{GeV/c^2}$ and $m_b = 4.95\,\mathrm{GeV/c^2}$) and with the CTEQ-4D [18] and GRV-LO [19] structure functions for the proton and photon, respectively. Allowing the contributions for beauty and charm plus light flavours to vary, a fraction of $(20 \pm 6\ (stat.)\ ^{+12}_{-7}\ (syst.)\ )\%$ for beauty production was determined. Using this value, the beauty production cross section, measured in the kinematic range $Q^2 < 1\,\mathrm{GeV}^2$, $0.2 < y < 0.8$, $E_T^{jet1} > 7\,\mathrm{GeV}$, $E_T^{jet2} > 6\,\mathrm{GeV}$, $|\eta^{jet}| < 2.4$, $p_T^{e^-} > 1.6\,\mathrm{GeV/c}$, and $|\eta^{e^-}| < 1.1$, was determined as

$$\sigma^{vis}_{b\bar{b}}(e^+\ p \to \text{dijet}\ e^-\ X) = \left(39 \pm 11\ (stat.)\ ^{+23}_{-16}\ (syst.)\ \right)\mathrm{pb}, \text{ZEUS preliminary}$$

The measured $b\bar{b}$ cross section is compared to leading order QCD Monte Carlo

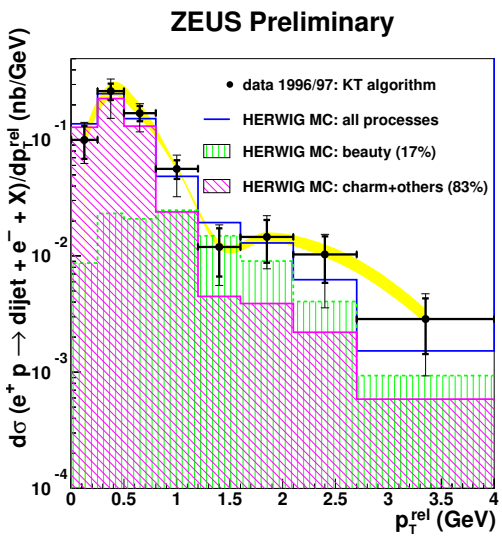

Fig. 5. The differential cross section in $p_{T,rel}$ for dijet events with an electron. The ZEUS data points are compared to the HERWIG Monte Carlo, which was scaled by a factor 3.7 to match the data. A beauty fraction of 17% is the HERWIG prediction.

predictions in figure 6 as a function of the b-quark mass assumed in the simulation. The HERWIG cross section decreases with mass and shows only a small dependence on the choice of the proton and photon structure function. The PYTHIA [20] program contains massless matrix elements and was used with the

GRV94-LO and GRV-LO [19] parton distributions functions for the proton and photon, respectively. It predicts a higher $b\bar{b}$ cross section than HERWIG. Due to the large errors, the present measurement cannot rule out either prediction.

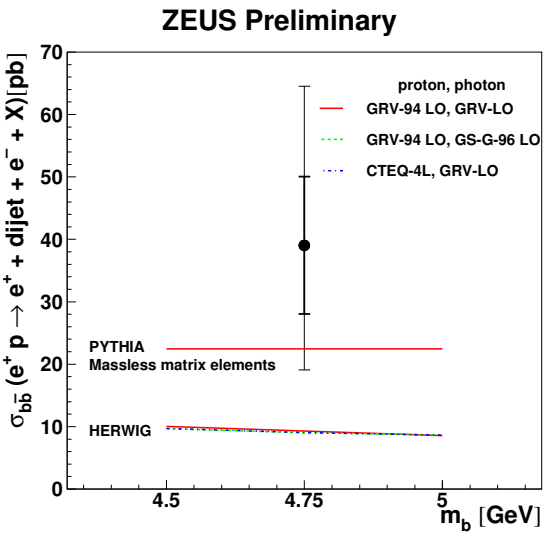

Fig. 6. The measured cross section for $b\bar{b}$ production with two jets and an electron in the final state, in the kinematic range specified in the text, compared to the HERWIG Monte Carlo with massive matrix elements and different proton and photon parton densities and to the PYTHIA Monte Carlo with massless matrix elements.

Further insight in the production mechanism for heavy quarks can be gained by measuring the differential cross section in the variable

$$x_\gamma^{obs} = \frac{\sum_{2jets} E_T^{jet}\, e^{-\eta^{jet}}}{2yE_e},$$

where E_e is the energy of the incoming positron. It is the fraction of the photon's momentum contributing to the production of the two jets. Direct processes involving pointlike photons are observed at $x_\gamma^{obs} \approx 1$, whereas resolved processes involving the partonic structure of the photon lead to smaller values.

Figure 7 shows the measured cross section $d\sigma/dx_\gamma^{obs}$ for events with two jets and an electron in the final state. It has a maximum at high x_γ^{obs} and a significant tail at low x_γ^{obs} which cannot be explained by direct processes and resolution effects alone. The HERWIG Monte Carlo predicts a 40% contribution from resolved photon processes, which, when added to the directed photon processes, provide a good description of the shape of the measured cross section. The overall normalization was scaled by a factor 3.7 to match the data. Fitting the ratio of resolved to direct photon processes yields a resolved contribution

of $(35 \pm 6\ (stat.))\%$ which is consistent with the HERWIG prediction and with the value measured in charm production [21]. A similar result is obtained when the measured cross section is compared to the PYTHIA Monte Carlo generator, which predicts a resolved contribution of 48%.

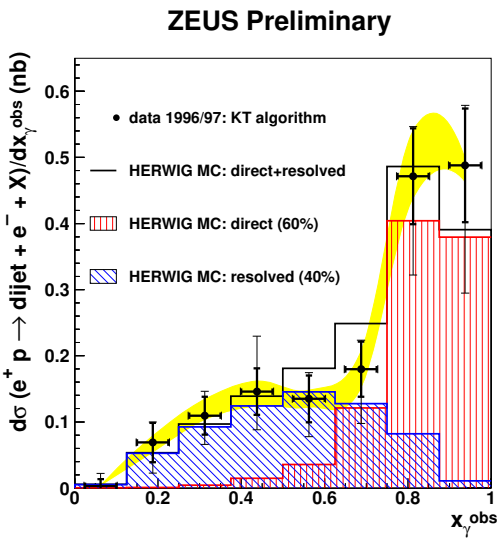

Fig. 7. The differential cross section in x_γ^{obs} for dijet events with an electron. The ZEUS data points are shown with statistical errors and with statistical and systematic errors added in quadrature. The shaded band shows the uncertainty due the calorimeter energy scale separately. The HERWIG prediction for direct and resolved contributions was scaled by a factor 3.7 to match the data.

4 Conclusions

The first measurements of open b photoproduction have been reported by H1 and ZEUS. Both experiments find cross sections that are about a factor of 4 larger than the expectations from leading order Monte Carlo Generators with massive matrix elements. The cross sections are measured in a visible range that involves the kinematics of the decay lepton. A comparison to next-to-leading order QCD calculations at the parton level requires an extrapolation to the full kinematic range or the addition of fragmentation and weak decays to the calculations. Both approaches add further systematic errors. The second approach has been followed by H1, which finds a cross section significantly larger than the NLO expectation.

The b purity is 50% for the H1 muon analysis and 20% for the ZEUS electron analysis. A higher purity can be obtained by using lifetime information from

existing or future silicon vertex detectors. It would allow a study of the resolved photon contribution to b photoproduction.

At higher Q^2 the present data samples should allow the first observation of open b production in deep inelastic scattering. A significant measurement of the structure function $F_2^b(x,Q^2)$, however, requires the increased luminosity expected from the HERA upgrade.

References

1. S. Frixione, M.L.Mangano, P. Nason, G. Ridolfi in *Heavy Flavours II*, ed. by A.J. Buras and M. Lindner, World Scientific, 1998
2. G. Ingelman, J. Rathsman, G.A. Schuler, Comp. Phys. Comm. 101 (1997) 135
3. R.K. Ellis, P. Nason, Nucl. Phys. B312 (1989) 551
4. J. Smith, W.L. van Neerven, Nucl. Phys. B374 (1992) 36
5. S. Frixione et al., Phys. Lett. B348 (1994) 633
6. U. Langenegger, to appear in *QCD and High Energy Hadronic Interactions. Proceedings, 33rd Rencontres de Moriond*, Les Arcs, France, March 1998
   G. Tsipolitis, in *Deep Inelastic Scattering and QCD. Proceedings, 6th International Workshop, DIS'98*, Brussels, Belgium, April 4–8, 1998, ed. by G. Coremans and R. Roosen, World Scientific, 1998
   H1 Collaboration, contributed paper no. 575 to the 29th International Conference on High Energy Physics, ICHEP'98, Vancouver, Canada, July 23-29, 1998
7. H1 Collaboration, C. Adloff et al., Phys. Lett. B467 (1999) 156
8. F. Jacquet, A. Blondel in *Proceddings of the Study of an ep facility for Europe*, ed. by U. Amaldi, DESY 79-48 (1979) 391
9. A.D. Martin, R.G. Roberts, W.J. Stirling, Phys. Lett. B354 (1995) 155
10. H. Jung, Comp. Phys. Comm. 86 (1995) 147
11. S. Frixione, M.L.Mangano, P. Nason, G. Ridolfi, Phys. Lett. B348 (1995) 348
12. M. Glück, E. Reya, A. Vogt, Phys. Rev. D46 (1992) 1973
13. EMC Collaboration, J.-J. Aubert et al., Phys. Lett. B106 (1981) 419
14. A.D. Martin, R.G. Roberts, W.J. Stirling, R.S. Thorne, Eur. Phys. J. C4 (1998) 463
15. M. Hayes, in *34th Rencontres de Moriond on QCD and Hadronic Interactions*, March 20-27, 1999, Les Arcs, France, and hep-ex/9905033
    M. Wing, in *7th International Workshop on Deep Inelastic Scattering and QCD*, April 19-23, 1999 , Zeuthen, Germany, and hep-ex/9905051
    ZEUS Collaboration, contributed paper no. 498 to the International Europhysics Conference on High Energy Physics, Tampere, Finland, July 1999
16. S. Catani, Y.L. Dokshitzer, B.R. Webber, Phys. Lett. B285 (1992) 291
17. G. Marchesini et al., Comp. Phys. Comm. 67 (1992) 465
18. H.L. Lai et al., Phys. Rev. D55 (1997) 1280
19. M. Glück, E. Reya, A. Vogt, Phys. Rev. D45 (1992) 3986
20. H.-U. Bengtsson, T. Sjöstrand, Comp. Phys. Comm. 46 (1987) 43
21. ZEUS Collaboration, J. Breitweg et al., Eur. Phys. J. C6 (1999) 67